

Submitted to J. Eur. Ceram. Soc.

Improvement of strength and reliability of ceramics by shot peening and crack-healing

Koji Takahashi ^a, Yoshitada Nishio ^b, Yoshiki Kimura ^b, Kotoji Ando ^a

^a Faculty of Engineering, Yokohama National University, 79-5, Tokiwadai,
Hodogaya, Yokohama, 240-8501, Japan

^b Graduate Student, Yokohama National University, 79-5, Tokiwadai, Hodogaya,
Yokohama, 240-8501, Japan

Correspondence:

Dr. Koji Takahashi
Faculty of Engineering,
Yokohama National University,
79-5, Tokiwadai, Hodogaya, Yokohama, 240-8501, Japan.
E-mail: ktaka@ynu.ac.jp

Improvement of strength and reliability of ceramics by shot peening and crack-healing

ABSTRACT

In this study we propose a new method for improving the surface strength and reliability of ceramics that combines shot peening with crack-healing ability. We used $\text{Si}_3\text{N}_4/\text{SiC}$ composite ceramics with high crack-healing ability and subjected the specimens to shot peening and crack healing. To evaluate the effect of our method, we investigated the residual stress after shot peening and crack healing and examined the specimens' mechanical properties, including apparent fracture resistance, contact strength and bending strength. We found that shot peening and crack-healing is effective to increase apparent fracture resistance, contact strength and bending strength.

KEY WORDS

Crack-healing, Shot peening, $\text{Si}_3\text{N}_4/\text{SiC}$, Residual stress, Contact strength, Ring crack

INTRODUCTION

Ceramics are candidate materials for industrial applications because of their excellent mechanical, tribological and thermal properties. These applications include bearings, turbo charger rotors, diesel engine components and cutting tools. However, because ceramics are brittle materials, fracture toughness is lower than that of metallic materials, resulting in lower reliability in mechanical properties. Thus, if the brittleness of ceramics is overcome, the reliability and product life of ceramic components will be improved. Many studies have been carried out to overcome the low fracture toughness of ceramics by (a) toughening the ceramic by fiber or whisker reinforcement, and microstructure control, and (b) activating the crack-healing ability to heal surface cracks introduced during machining and service.

Significant progress has been made in the area of toughening by fiber or whiskers [1], while there have been fewer studies involving crack-healing ability, though the number of works is still increasing [2-15]. The proposed mechanisms of crack healing have been described by many researchers. Among the several types of crack healing, that induced by the oxidation of silicon carbide (SiC) has advantages, because the complete recovery of strength is attained by this mechanism. The SiC oxidation concept was proposed by Ando and colleagues [7,8]. Since then, there have been many reports on crack-healing behavior of $\text{Si}_3\text{N}_4/\text{SiC}$ [8,9,12], Mullite/SiC [7,13], $\text{Al}_2\text{O}_3/\text{SiC}$ [10,11] and SiC/AlN [14].

Shot peening is a common procedure used to increase the near-surface strength of metals [16]. In the shot-peening process, a stream of small, hard spheres is shot at a treated surface. Compressive residual stress is generated by the localized plastic deformation of the surface layer. Fatigue strength of metals can be increased by shot peening, because the compressive residual stress prevents fatigue crack initiation and propagation [16,17]. Although researchers believed that strengthening of ceramics due to shot peening would not be possible, recent studies show that the near-surface strength of ceramics can be improved by shot peening [18-21].

Pfeiffer and Frey carried out shot peening on alumina and silicon nitride by using 0.61- to 0.69-mm tungsten carbide shots [18,19]. They reported that high compressive residual stress up to more than 1 GPa could be introduced near the surface and the compressive residual stress improved the near-surface strength of ceramics. Moon et al. reported that apparent fracture resistance at the sub-surface of alumina and silicon nitride was increased by shot peening [20]. Tanaka et al. carried out shot peening on silicon nitride using 0.05-mm high-strength steel shots and 1.1-mm tungsten carbide shots [21]. They reported that compressive residual stress up to 1.5 GPa was introduced near the surface, and the compressive residual stress increased the apparent fracture resistance at sub-surface up to 2.5-fold.

Considering the results obtained in previous studies, the shot peening of ceramics is a promising technique for increasing strength in the surface region. Strengthening the surface layer will increase the contact strength of ceramic components such as bearings and turbine blades in which higher contact strengths are desirable. However, if surface cracks are unintentionally induced during the machining and shot peening process, the reliability of the ceramics components will be decreased. If crack healing is used in combination with shot peening, increasing the surface strength and reliability of ceramics will be achieved simultaneously. In this study we propose a new method for improving the strength and reliability of ceramics that combines shot peening with crack-healing ability. The effects of shot peening and crack healing on the residual stress, apparent fracture resistance at sub-surface, contact strength and bending strength were investigated.

EXPERIMENTAL PROCEDURES

Material and specimens

In this study, we used silicon nitride reinforced by silicon carbide ($\text{Si}_3\text{N}_4/\text{SiC}$) [8,9,12] which has excellent crack-healing ability. The Si_3N_4 powder used in this study has a mean particle size of 0.2 μm . The SiC powder used has a 0.27- μm mean particle size. The samples were prepared using a mixture of Si_3N_4 with 20 wt% SiC powder and 8 wt% Y_2O_3 as a

sintering additive powder. The Y_2O_3 powder used has a 0.4- μm mean particle size. To this mixture, alcohol was added, and the mixture was blended completely for 48 h. The mixture was placed in an evaporator to extract the solvent and then in a vacuum to produce a dry powder mixture. The mixture was subsequently hot-pressed at 1850°C and 35 MPa for 2 h in an N_2 atmosphere. The relative density of the hot-pressed material determined by the Archimedes method was 99.5% of the theoretical density (3.32 kgf/mm³). The average grain size of the matrix was $Si_3N_4=0.44 \mu m$, and the average aspect ratio was about 5.0. Most SiC particles were located in grain boundaries and distributed uniformly. This material was selected as a test material because it has an excellent crack-healing ability. The hot-pressed plate was then cut into test specimens measuring 3×4×22 mm. The specimens were polished to a mirror finish on one face.

Shot peening and residual stress

Shot peening was carried out on the Si_3N_4/SiC specimens with a direct pressure peening system. Three specimens were shot peened simultaneously. The zirconium oxide (ZrO_2) beads with a diameter 0.3 mm were used. The peening pressure was 0.2 MPa. Peening time was 40s for three specimens. The resulting Almen-intensity was 0.16 mmA. The specimens subjected to shot peening are called “SP” specimens, and the specimens without shot peening are called “Non-SP” specimens. After shot peening, specimens were heat-treated in air for 1 or 5 h at temperatures from 500 to 1400 °C so we could investigate the effects of heat treatment on residual stress, apparent fracture resistance, contact strength and bending strength. These specimens are called “SP + heat-treated” specimens. The residual stresses were measured for Non-SP, SP and SP + heat-treated specimens by the X-ray diffraction method. The conditions for X-ray diffraction are shown in **Table 1**. To investigate the in-depth residual stress distribution, we removed the surface layers by polishing the specimens with diamond abrasives of 9.0, 3.0 and 0.5 μm . We confirmed that removal of the surface layers resulted in negligible residual stress.

Measurement of apparent fracture resistance, contact strength and bending strength

For measurement of apparent fracture resistance at sub-surface, Non-SP specimens, SP specimens and SP + heat-treated specimens were prepared. To prepare SP + heat-treated specimens, the SP specimens were heat treated in air for 1 h at 900 – 1300 °C. The apparent fracture resistance (K_c) was evaluated by the indentation-fracture (IF) method, in which apparent fracture resistance can be estimated using the following equation in accordance with Japan Industry Standards (JIS) [22]:

$$K_C = 0.026E^{1/2}P^{1/2} \frac{a}{c^{3/2}} \quad (1)$$

where E is Young's modulus, P is the indent load, a is half the diagonal length of indentation and c is half the surface crack length. Vickers indentations were introduced on the polished surface by applying an indent load of 49 N for 20 s. The Young's modulus of the material is $E = 300$ GPa. Note that the value of fracture resistance (K_C) is affected by residual stress [23]. For comparison, we evaluated the intrinsic fracture toughness (K_{IC}) of the Non-SP specimens using the single-edge V notch beam (SEVNB) method. The V notch was made on the bending test specimens where the V notch shape was as follows: depth = 1.2 mm, notch angle = 20°, notch root radius = 0.04 mm.

For measurement of contact strength, Non-SP, SP and SP + heat-treated specimens were prepared. To prepare SP + heat-treated specimens, the SP specimens were heat treated in air for 1 h at 900 – 1300 °C. The contact strength was measured by sphere indentation tests, as shown in **Fig. 1**. Indentations were made on the surface of the specimens using tungsten carbide (WC) spheres with a diameter of 4 mm, to prescribed loads at a crosshead speed of 0.2 kN/min. After unloading the loads, the indented surfaces were observed by optical microscopy to identify a crack initiation. Three specimens were used for indentation tests. We compared the critical load P_c where the crack initiation did not occur in all three specimens.

For measurement of bending strength, Non-SP, SP and SP + heat-treated specimens were prepared. A Vickers indentation was made on the center of the polished face of the Non-SP, SP and SP + heat-treated specimens at loads of 19.6 to 98.0 N to simulate the surface cracks introduced by shot peening or other contact events. These specimens are called “Non-SP + cracked”, “SP + cracked” and “SP + heat-treated + cracked” specimens, respectively. Some SP + cracked specimens and Non-SP + cracked specimens were heat treated in air at 1100°C for 5 h to investigate the effects of shot peening on the crack healing process. These specimens are called “SP + cracked + heat-treated” and “Non-SP + cracked + heat-treated” specimens. The specimens were subsequently tested in three-point bending at a crosshead speed of 0.5 mm/min, using a fixture with a span of 16 mm.

EXPERIMENTAL RESULTS AND DISCUSSION

Residual stress

Figure 2 shows the residual stress distributions induced by SP. The maximum compressive residual stress of 880 MPa was observed at the surface. The compressive residual stress decreased in-depth direction. The compressive residual stress was induced approximately up to 40 μm.

Figure 3 shows residual stress at the surface as a function of heat treatment temperature. Compressive residual stress decreased as the heat treatment temperature was increased. However, the specimen heat treated at 800-1100 °C showed compressive residual stresses of 300-400 MPa. In Si₃N₄/SiC, crack healing occurs above 800 °C. Thus, inducing compressive residual stress and crack healing were used simultaneously.

Compressive residual stress in the surface layer may reflect the volume expansion induced by micro-crack initiation within crystallites. The lattice strain was relieved due to thermal expansion as a result of increasing the heat treatment temperature. Crack-healing due to oxidation of SiC occurs above 800 °C. The oxidation of SiC includes approximately 80% volume expansion of the condensing phase [15]. The oxidation products fill the micro-cracks, which leads to a volume expansion at the surface. Thus, the relaxation of compressive residual stress was not pronounced at 800-1100 °C. On the other hand, the lattice strain was eliminated due to softening the grain boundary glassy phase above 1200°C.

Vickers indentation cracks and surface condition

Figure 4 shows the optical micrograph of Vickers indentation and cracks for Non-SP and SP specimens. The Vickers indentation load was 98 N. Cracks were clearly observed in Non-SP specimens, as shown in Fig. 4(a), whereas the surface cracks were very short in SP specimens, as shown in Fig. 4(b). **Table 2** shows the length of surface cracks for Non-SP +cracked, SP + cracked and SP + heat-treated + cracked specimens. The lengths of surface cracks in SP + cracked and SP + heat-treated + cracked specimens were much smaller than that of SP + cracked specimens. It is clear that the compressive residual stress increases the resistance to crack initiation at sub-surface.

The maximum height of roughness for Non-SP specimens and SP specimens was $R_y = 0.24 \mu\text{m}$ and $0.30 \mu\text{m}$, respectively. Thus, the surface condition was not changed greatly by the shot peening.

Apparent fracture resistance

Figure 5 shows the apparent fracture resistance (K_C) at sub-surface measured by the IF method. The average value of fracture toughness (K_{IC}) for Non-SP specimens measured by the SEVNB method was $4.9 \text{ MPam}^{1/2}$. Thus, the value of K_C of the Non-SP specimens measured by the IF method ($K_C = 4.1 \text{ MPam}^{1/2}$) is close to the K_{IC} of the material. The K_C of the SP specimens increased 2.3-fold in contrast to the K_C for the Non-SP specimens. After heat treatment, the K_C for the SP specimens decreased. However, if the heat treatment temperature was 800 – 1100 °C, at which crack healing is possible, the K_C after heat treatment was more than 2 times as great. If the healing temperature was 1300 °C, the value of K_C was

the same for the SP and Non-SP specimens. Thus, increasing the K_C is closely related to compressive residual stress.

Contact strength

Figure 6 shows the results of sphere indentation tests. The open circles indicate that no ring-crack was observed on the surface of specimens, whereas the solid triangles indicate that a ring-crack was observed. The critical loads P_c for crack initiation are shown by left-pointing arrows. The P_c for Non-SP specimens was 0.5 kN, whereas the P_c for SP specimens was more than 4.5 kN, which was the maximum load of the testing system. Thus, the P_c increased more than 9 times by shot peening. The P_c for the SP + heat-treated specimens decreased with increasing heat-treatment temperature. The tendency of decreasing P_c with increasing heat-treatment temperature is similar to that of K_C . This is because both K_C and P_c are closely related to the compressive residual stress. We noted that the P_c of SP + heat-treated specimens was 4 times greater than that of the Non-SP specimens if the heat treatment temperature was 1100 °C, at which crack-healing is possible.

Bending strength

Figure 7 shows the bending strength as a function of Vickers indentation load. The bending strength of Non-SP + cracked specimens (solid triangles) decreased steeply with increasing Vickers indentation loads, although the decrease rates of the bending strength of SP + cracked specimens (solid inverse triangles) and SP + heat-treated + cracked specimens (solid diamonds) were smaller than that of Non-SP + cracked specimens. The main reason for this is that the lengths of surface cracks in SP + cracked specimens and SP + heat-treated + cracked specimens were much shorter than that of Non-SP + cracked specimens, as shown in Table 2. We note that the bending strengths of SP + heat-treated + cracked specimens were higher than those of SP + cracked specimens. Similarly, the bending strength of SP + heat-treated specimens (open triangle) was higher than that of the SP specimens (open inverse triangles). As mentioned already, the compressive residual stress decreased due to heat-treatment, as shown in Fig. 3. Thus, the increase of bending strength was due to healing of small surface cracks produced by the shot peening process. These results indicate that the shot peening in combination with crack healing increased the strength at the sub-surface of the test material.

If the indentation load was less than 49 N, the bending strength of SP + cracked + heat-treated specimens (solid squares) and Non-SP + cracked + heat-treated specimens (open circles) had recovered, and these specimens showed bending strength similar to each other and close to the strength of the specimens with no indentations. Most of the specimens fractured outside the crack-healed zone. As the indentation load was increased to 98 N, the

bending strengths of SP + cracked + heat-treated specimens were higher than those of the Non-SP + cracked + heat-treated specimens. The difference of bending strength was caused by the difference of the crack length, as shown in Table 2. Thus, the effect of the shot peening on the crack healing process increased as the indentation load increased.

CONCLUSION

We investigated the effects of shot peening and crack-healing on residual stress, apparent fracture resistance, contact strength and bending strength of Si₃N₄/SiC composite. The results are summarized as follows:

- (1) The maximum compressive residual stress of 880 MPa was observed at the surface. The compressive residual stress was induced to approximately 40 μm in depth.
- (2) The apparent fracture resistance at the sub-surface was improved by a shot peening factor of 2.3.
- (3) The contact strength of Si₃N₄/SiC was increased more than 9 times by shot peening.
- (4) After heat treatment, the apparent fracture resistance and contact strength of SP specimens decreased. However, if the heat treatment temperature was 800 – 1100 °C, at which crack healing is possible, the apparent fracture resistance and contact strength showed very high values.
- (5) The decrease rates of the bending strength against Vickers indentation loads of SP + cracked specimens and SP + heat-treated + cracked specimens were smaller than that of Non-SP + cracked specimens. The reason for this is that the surface cracks induced in SP + cracked and SP + heat-treated + cracked specimens were much shorter than those of Non-SP + cracked specimens.
- (6) The bending strengths of SP + heat-treated + cracked specimens were higher than those of SP + cracked specimens. Similarly, the bending strength of SP + heat-treated specimens was higher than that of the SP specimens. The increase of bending strength was due to healing of small surface cracks produced by the shot peening process.
- (7) As the indentation load increased to 98 N, the bending strengths of SP + cracked + heat-treated specimens were higher than those of the Non-SP + cracked + heat-treated specimens. Thus, the effect of the shot peening on the crack healing process increased as the indentation load increased.
- (8) Considering the experimental results of (1) to (7), we conclude that shot peening in combination with crack healing is a useful technique to improve the strength and reliability of ceramics.

ACKNOWLEDGMENTS

The authors thank Mr. Keita Takahashi and Dr. Shinji Saito for their assistance with the experimental program. This study was supported by Grant-in-Aid for Young Scientists (B) (No. 18760077) from the Ministry of Education, Culture, Sports, Science and Technology of Japan.

REFERENCES

1. Green D.J., *An Introduction to the Mechanical Properties of Ceramics*, Cambridge University Press, Cambridge, 1998, pp. 248-264.
2. Petrovic, J.J. and Jacobson, L.A., Controlled surface flaws in hot-pressed SiC, *J. Am. Ceram. Soc.*, 1976, 59[1-2], 34-37.
3. Choi, S.R. and Tikare, V., Crack healing behavior of hot pressed silicon nitride due to oxidation, *Scr. Metall. et Mater.*, 1992, 26, 1263-1968.
4. Zhang, Y.Z., Edwards, L. and Plumbridge, W.J., Crack healing in a silicon nitride ceramics. *J. Am. Ceram. Soc.*, 1998, 81, 1861-1868.
5. Chu, M.C., Cho, S.J., Lee, Y.C., Park, H.M. and Yoon, D.Y., Crack healing in silicon carbide, *J. Am. Ceram. Soc.*, 2004, 87(3), 490-492.
6. Chlup, Z., Flasar, P., Ando, K., Dlouhy, I., Fracture behaviour of Al₂O₃/SiC nanocomposite ceramics after crack healing treatment, *J. Eur. Ceram. Soc.*, 2008, 28, 1073-1077.
7. Chu, M. C., Sato, S., Kobayashi, Y. and Ando, K., Damage healing and strengthening behavior in intelligent Mullite/SiC ceramics, *Fatigue Fract. Eng. Mater. Struct.*, 1995, 18(9), 1019-1029.
8. Ando, K., Ikeda, T., Sato, S., Yao, F. and Kobayashi, Y., A preliminary study on crack healing behaviour of Si₃N₄/SiC composite ceramics. *Fatigue Fract. Engng. Mater. Struct.*, 1998, 21, 119-122.
9. Ando, K., Takahashi, K., Nakayama, S. and Saito, S., Crack-healing behavior of Si₃N₄/SiC ceramics under cyclic stress and resultant fatigue strength at the healing temperature. *J. Am. Ceram. Soc.*, 2002, 85 (9) 2268-2272.
10. Ando, K., Kim, B.S., Chu, M.C., Saito, S. and Takahashi, K., Crack-healing and mechanical behavior of Al₂O₃/SiC composites at elevated temperature, *Fatigue Fract. Eng. Mater. Struct.*, 2004, 27, 533-541.
11. Takahashi, K., Yokouchi, M., Lee, S.K., Ando, K., Crack-healing behavior of Al₂O₃ toughened by SiC whiskers, *J. Am. Ceram. Soc.*, 2003, 86(12), 2143-2147.
12. Takahashi, K., Ando, K., Murase, H., Nakayama, S. and Saito, S., Threshold stress for crack-healing of Si₃N₄/SiC and resultant cyclic fatigue strength at the healing temperature, *J. Am. Ceram. Soc.*, 88, 2005, 645-651.
13. Takahashi, K., Uchiide, K., Kimura, Y., Nakao, W., Ando, K. and Yokouchi, M., Threshold stress for crack-healing of mullite reinforced by SiC whiskers and SiC particles and resultant fatigue strength at the healing temperature, *J. Am. Ceram. Soc.*, 2007, 90(7), 2159-2164.
14. Magnani, G., Beaulardi, L., Brentari, A., Toyoda, T. and Takahashi, K., Crack healing in liquid-phase-pressureless-sintered silicon carbide-aluminum nitride composites, *J. Eur. Ceram. Soc.*, 2010, 30(3), 769-773.
15. Nakao, W., Takahashi, K. and Ando, K., Self-healing of surface cracks in structural ceramics, In *Self-Healing Materials: Fundamentals, Design Strategies, and Applications*, eds. Ghosh, S.K., WILEY-VCH, Weinheim, 2009, pp. 183-217.
16. Suresh, S., In: *Fatigue of Materials*, Cambridge University Press, Cambridge, 1991, pp.134-135.

17. Takahashi, K., Ando, K., Amano, T., Miyamoto, T., Takahashi, F., Tange, A., Okada, H. Ono, Y., Improvement of bending fatigue limit by shot peening for spring steel specimens, containing an artificial surface defect, Proceedings of ICSP-10, 2008, 305-310.
18. Frey, T. and Pfeiffer, W., Shot peening of ceramics: Damage or Benefit?, In Shot Peening, ed. Wgner, L., WILEY-VCH , Weinheim, 2003, pp. 185-190.
19. Pfeiffer, W. and Frey, T., Strengthening of ceramics by shot peening, *J. Eur. Ceram. Soc.*, 26, 2006, 2639-2645.
20. Moon, W.J., Ito, T., Uchimura, S. and Saka, H., Toughening of ceramics by dislocation sub-boundaries, *Materials Science and Engineering A*, 387–389, 2004, 837–839.
21. Tanaka, K., Akiniwa, Y. and Morishita, Y., Residual stress distribution in the sub-surface region of shot-peened ceramics, *Transactions of the Japan Society of Mechanical Engineers A* , 71(712), 2005, 1714-1721.
22. Japan Industrial Standards R1607, Testing method for fracture toughness of fine ceramics, Japan Standards Association, 1995.
23. Hoshide, T., Estimation of residual stress with non-uniform distribution by indentation fracture method in ceramics, *Material Science Research International*, 4-4, 1998, 294-296.

Captions of tables and figures

Table 1. Conditions for X-ray diffraction.

Table 2. Length of surface cracks for Non-SP and SP specimens.

Figure 1. Schematic illustration and photograph of ring cracks on the surface of Non-SP specimen.

Figure 2. Relationship between residual stress and depth from surface.

Figure 3. Residual stress at the surface as a function of heat treatment temperature.

Figure 4. Optical photograph of Vickers indentation and cracks (Indented load: 98N), (a) Non-SP specimen, (b) SP specimen.

Figure 5. Relationship between surface treatment conditions and apparent fracture resistance.

Figure 6. Relationship between surface treatment conditions and sphere indentation load.

Figure 7. Relationship between indentation load and bending strength

Table1

Characteristic X ray	Cu-K α_1
X ray tube	Cu
Diffraction plane	Si ₃ N ₄ (323)
Diffraction angle [deg]	141.26
Tube voltage [kV]	40
Tube current [mA]	30

Table2

Vickers indentation load [N]	Length of the surface cracks $2c$ [μm]		
	Non-SP + cracked specimens	SP + cracked specimens	SP + heat-treated + cracked specimens
19.6	107.4	63.5	87.0
49.0	188.4	106.8	117.1
98.0	300.1	156.7	179.6

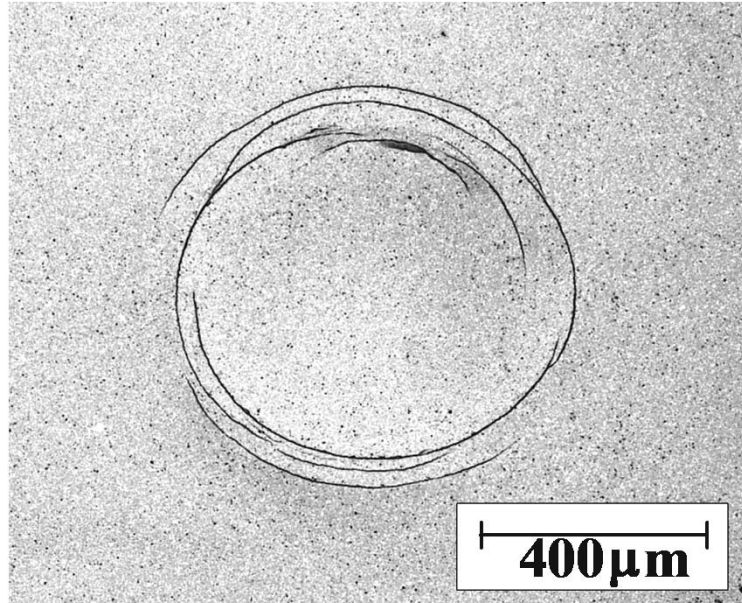


Fig.1

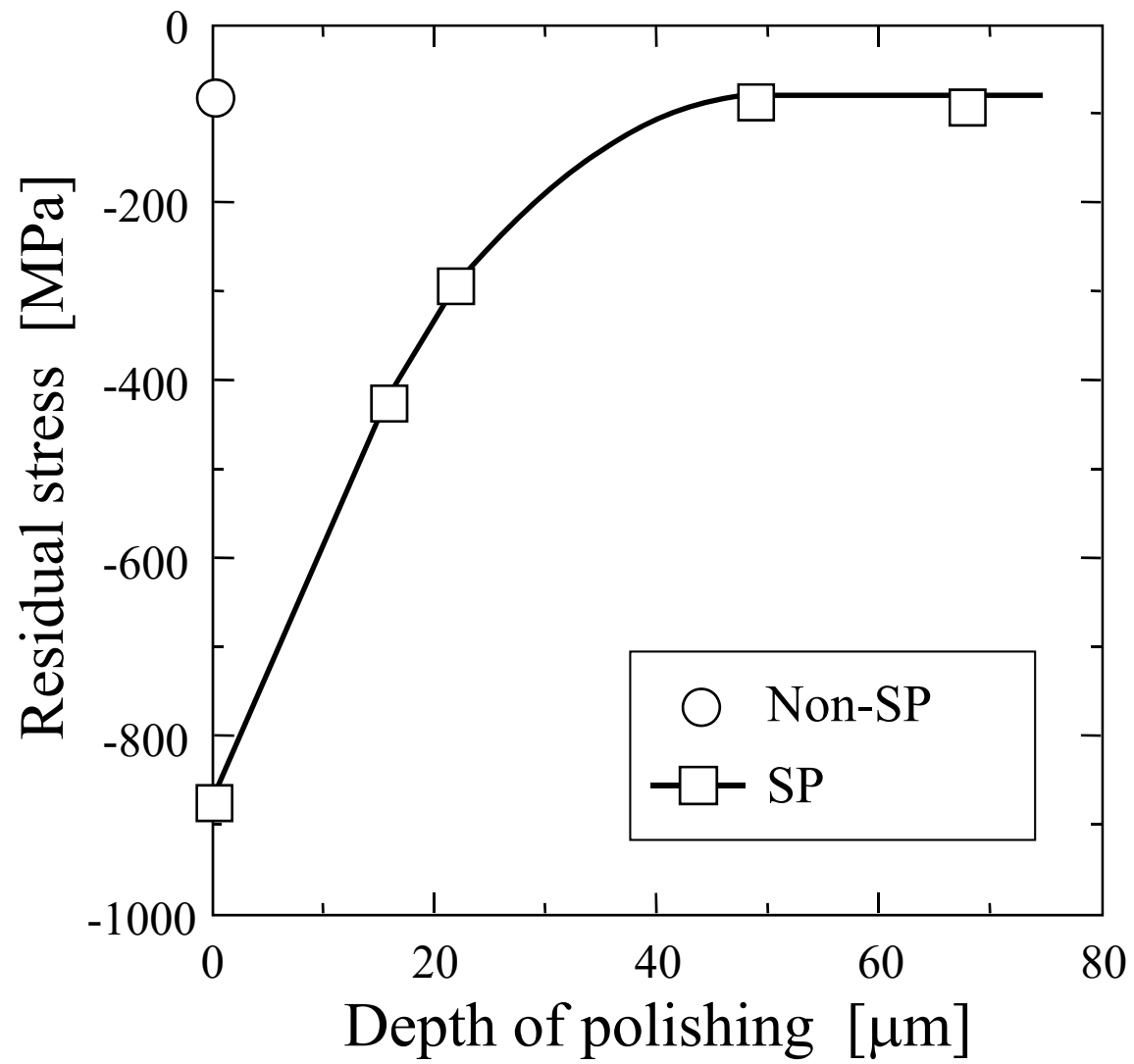


Fig.2

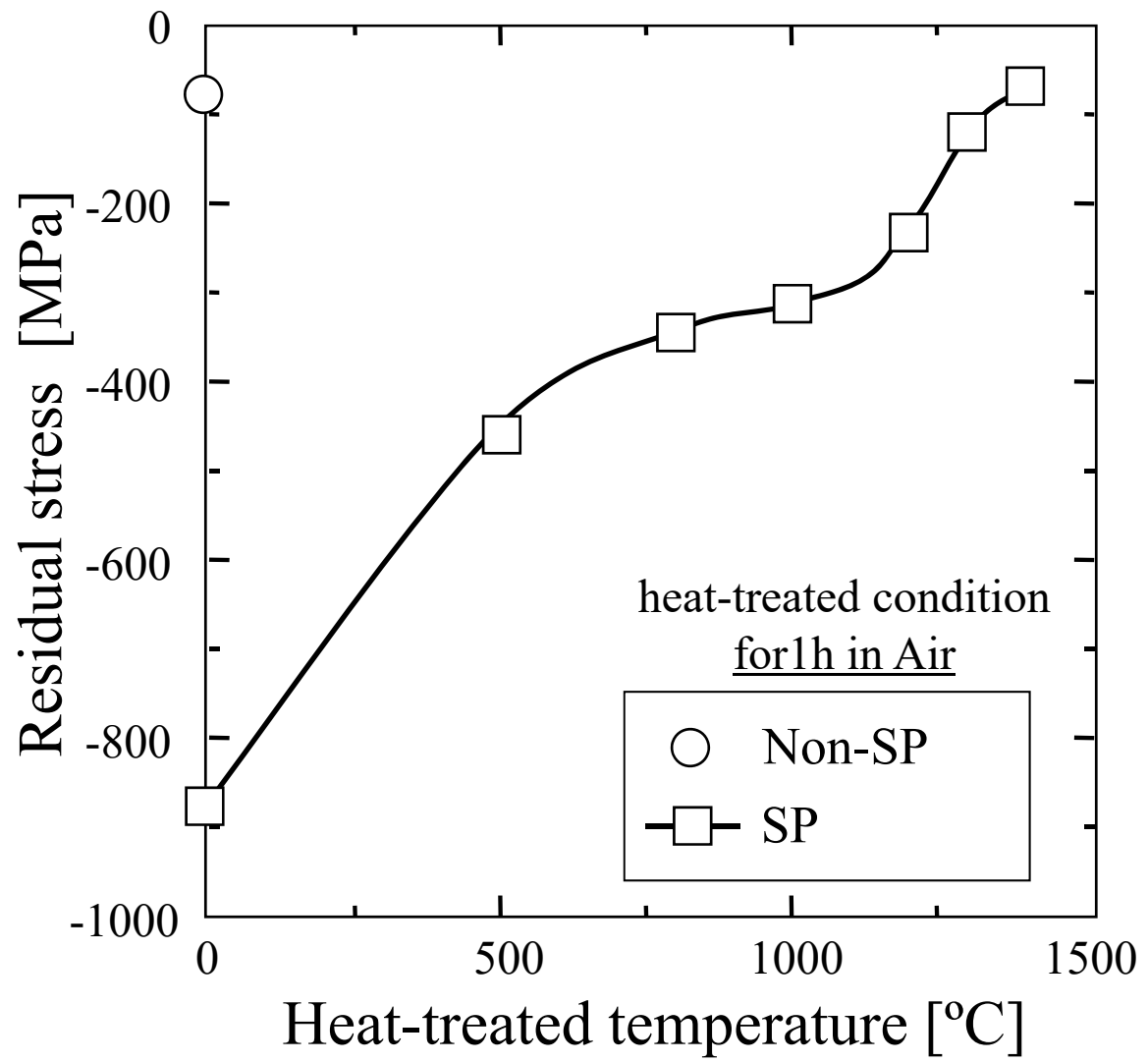


Fig.3

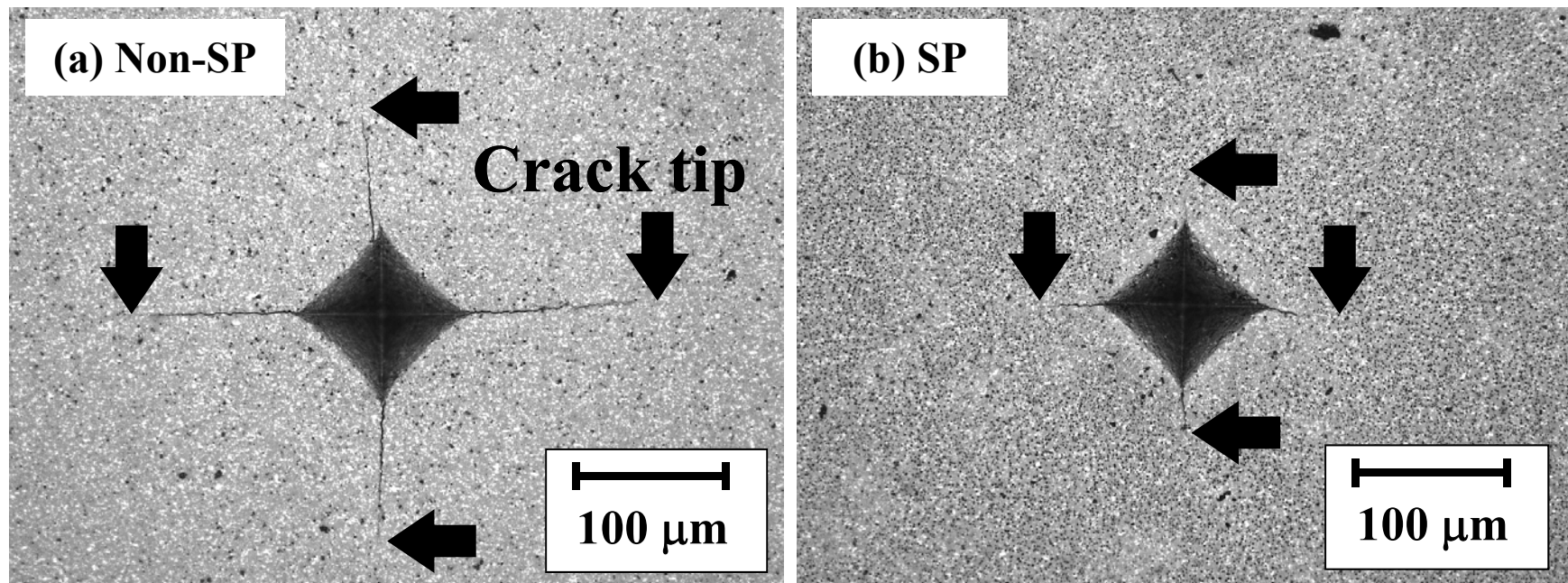


Fig.4

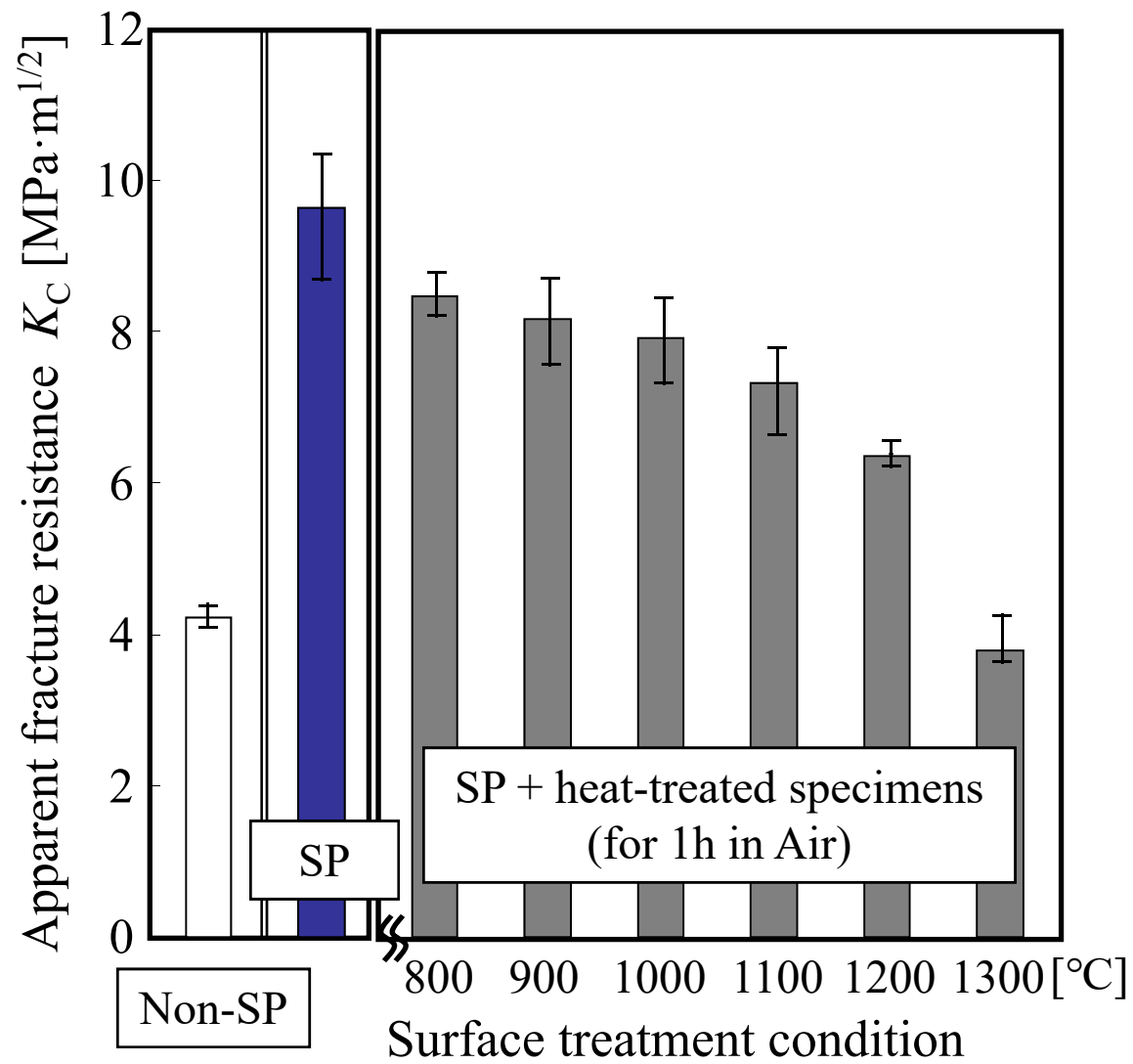


Fig.5

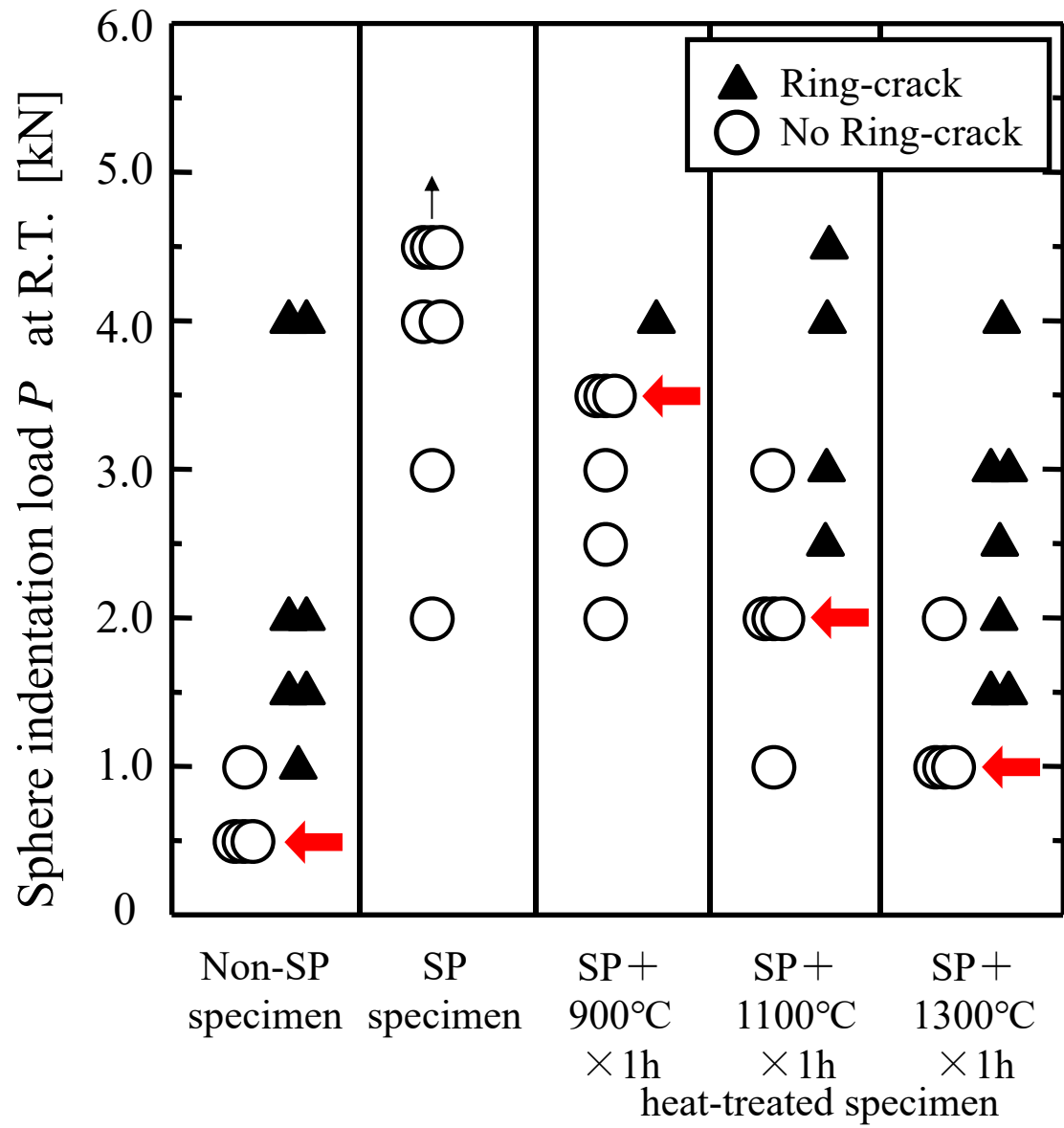


Fig.6

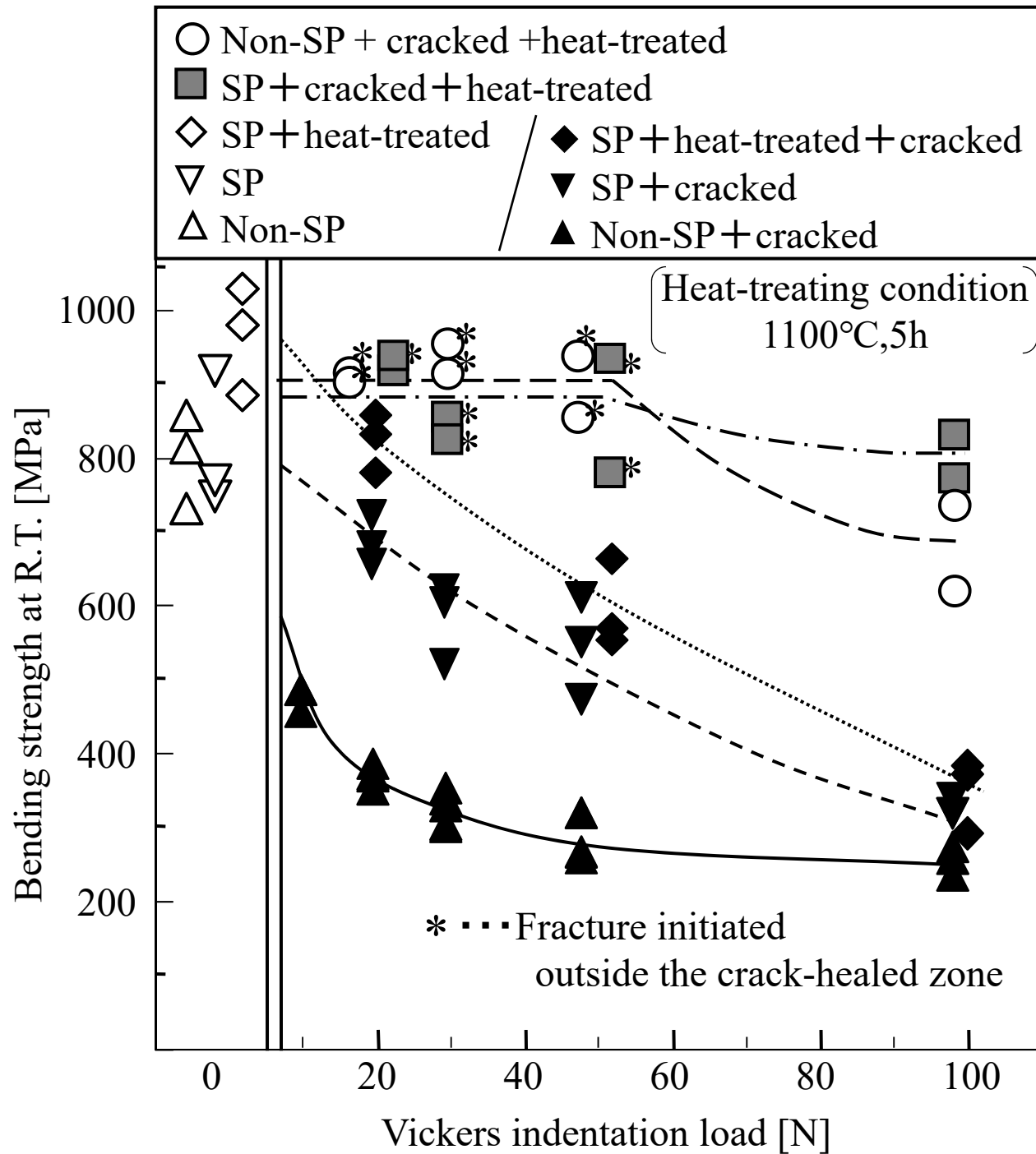


Fig.7